

Synchrotron Radiation Profile Monitor for the HERA Positron Beam

G. Kube, R. Fischer, and K. Wittenburg

Deutsches Elektronen-Synchrotron DESY, Notkestrasse 85, D-22603 Hamburg, Germany

Abstract. For the measurement of the positron beam emittance at the e-p storage ring HERA at DESY a monitor is used which is based on the direct imaging of visible synchrotron radiation from a bending magnet. While the resolution of profile measurements by synchrotron radiation is already strictly limited by inherent effects, the observation in off-axis geometry modifies the measured vertical angular intensity distribution additionally. As a result the beam image is broadened due to the increased contribution of the diffraction limited resolution. In the present article detailed calculations concerning the image resolution especially in view of off-axis observation are presented. Furthermore the calculations indicate that the influence of resolution broadening effects may be overestimated by the standard formulas used as rule of thumb.

INTRODUCTION

The precise determination of the beam emittance is essential for the understanding of luminosity in colliding beam experiments as the ones at the proton-positron storage ring HERA. While the emittance itself is no direct accessible quantity, the beam width is usually measured so that the emittance can be calculated based on the knowledge of beam optical parameters. For the measurement of the e^+ beam size at HERA a profile monitor is used which utilizes the visible part of synchrotron radiation (SR) from a bending magnet to form an image of the beam. The image resolution of this kind of monitor is affected by inherent effects like diffraction and depth of field. However, by careful calculations of these resolution broadening contributions, the real beam size can still be derived.

The development of a model to describe these influences has turned out to be nontrivial. Attempts range from rules of thumb to quite elaborate models, see Refs. [1, 2] and the references therein. The model presented in this article follows the outlines described in the references quoted above. Special emphasis is put on the discussion of resolution broadening influences in vertical direction due to off-axis observation, i.e. if a part of the radiation used for image formation is shielded. Examples are the usage of a slotted mirror as described in Ref. [3], or moving the mirror away from the beam axis in vertical direction as it is the case for the HERA monitor. The reason for is to reduce thermal heating of the light extracting mirror due to absorption of hard X-ray radiation which would result in an image deformation.

PROFILE MONITOR SETUP

In luminosity operation the HERA positron beam energy amounts to $E = 27.6$ GeV. According to the beam optical design parameters, in this mode the e^+ beam should have a horizontal (1σ) size of $\sigma_x = 1143 \mu\text{m}$ and a vertical one of $\sigma_y = 337 \mu\text{m}$. Task of the optical system is to provide an image of the beam onto the chip of the CCD camera.

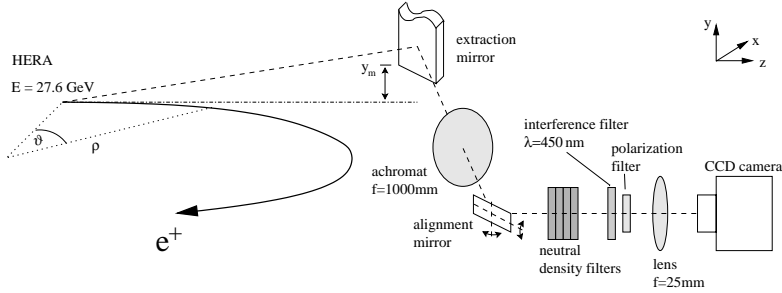


FIGURE 1. Schematic picture of the profile monitor setup.

In Fig. 1 a sketch of the monitor setup is shown. The emitted SR radiation is extracted out of the vacuum system by a mirror (thickness 2 mm, width 15 mm) which is located $\hat{p} = 6216$ mm away from the central part of the bending magnet. The mirror surface has an inclination angle of 45° with respect to the xy plane, hence the light is reflected out perpendicular to the beam axis. An achromatic lens with focal length $f = 1000$ mm, located $p = 6485.5$ mm away from the source point, forms an image in a distance $p' = 1182.3$ mm. The resulting real intermediate image is then magnified by a second lens ($f = 25$ mm) onto the chip of the CCD camera (*JAI CV-M300E* with 768×494 pixels of size $11.6 \times 13.5 \mu\text{m}^2$). The total magnification factor of the optical system amounts to $V = 0.55$. The video output of the camera is fed to a commercially available 8 bit PCI framegrabber board (*Data Translation DT3155*) for digitalization and finally analyzed by a standard personal computer.

In order to minimize chromatic errors and to improve the diffraction limited resolution an interference filter with central wavelength $\lambda = 450$ nm is used. With the polarization filter it is possible to select the horizontally (σ) or vertically (π) polarized light component in order to investigate the influence on the diffraction limited resolution. The neutral density filters serve to adjust the incoming light intensity to avoid saturation of the camera chip. The alignment mirror which is rotateable about the x and y axis allows for adjustment of the image in the center of the CCD.

The light extracting mirror is made of beryllium which has a high thermal conductivity together with a low absorption coefficient for hard X-rays. Thereby, a large part of the emitted SR spectrum with critical energy $\hbar\omega_c = 76$ keV will cross the mirror without absorption and reduce thermal heating. Additionally, the mirror is cooled by water. However, these precautions are not sufficient to reduce thermal heating down to a level that no mirror surface distortion occurs. The absorption of the low energetic part of the SR spectrum at the surface leads to a deformation of the beam image and even the destruction of the mirror. Therefore, in the normal operation mode of the monitor the

extracting mirror bottom edge is placed $y_m = 2 \dots 4$ mm above the beam axis. In this geometry the X-ray part of SR which is emitted close to the beam axis will not affect the mirror, while the optical SR components which are emitted under larger angles are reflected out of the vacuum system.

DIFFRACTION LIMITED RESOLUTION

The resolution broadening calculations are based on the approach of Hofmann and Méot [1] which starts from the assumption of spherical wave propagation through obstacles under the condition of scalar Fraunhofer diffraction. Consider a point source located in the origin of the source plane (x_0, y_0) which is imaged onto the origin of the image plane (x', y') , cf. Fig. 2.

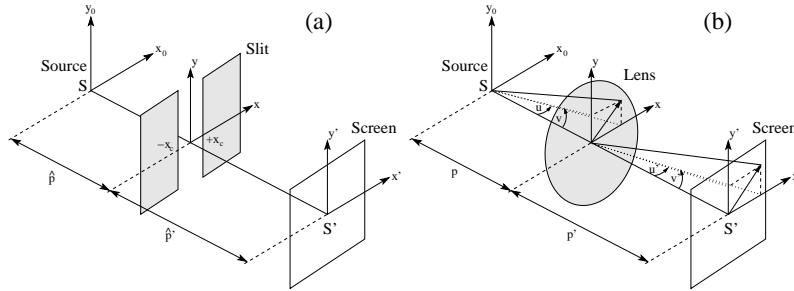


FIGURE 2. Geometry for the calculation of horizontal (a) and vertical (b) diffraction limited resolution.

The field distribution of the Fraunhofer diffraction pattern is determined by the Fourier transform of the source field distribution $f(x, y)$ over the aperture

$$F(x', y') = \iint_{\text{aperture}} f(x, y) e^{-ik(xx' + yy')/p'} dx dy = F_x(x') \times F_y(y'), \quad (1)$$

supposed the integrations in x, y over the limiting aperture can be carried out independently. $u' = x'/p'$, $v' = y'/p'$ are the emission angles in the image plane. From the amplitude distribution in the image plane the intensity distribution can be calculated by

$$I_x(x') = |F_x(x')|^2, \quad I_y(y') = |F_y(y')|^2. \quad (2)$$

Horizontal Distribution. In horizontal direction the aperture is defined by the horizontal dimensions of the light extracting mirror. As indicated in Fig. 2(a) the situation is similar to the diffraction at a slit aperture, while the slit width $w = 2|x_c|$ is defined by the projection of the mirror width onto the beam axis. According to Refs. [1, 2], the amplitude distribution f can be considered as uniform across the slit because of the circulating motion in the horizontal plane. The evaluation of Eq.(1) in x direction results in the diffraction pattern from a single slit

$$F_x(x') = 2x_c \operatorname{sinc} \left(\frac{2\pi u_{\max} x'}{\lambda \hat{V}} \right) \quad (3)$$

with the magnification $\hat{V} = \hat{p}'/\hat{p}$ and $u_{max} = x_c/\hat{p}$ the maximum angle in the horizontal plane. From Eq.(3) it is obvious that the diffraction limited resolution is mainly determined from the slit resp. the mirror width.

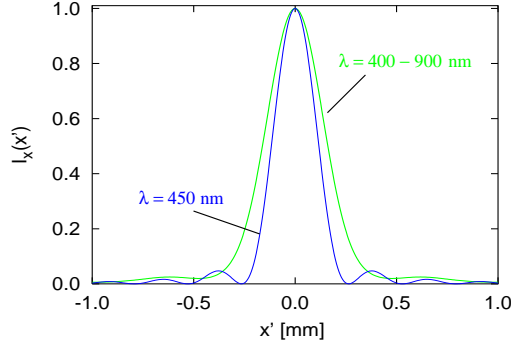


FIGURE 3. Diffraction limited normalized horizontal single electron intensity distribution $I_x(x') = |F_x(x')|^2$ of SR for the HERA profile monitor, assuming the field distribution of Eq.(3) with $\hat{V} = 1$.

Fig. 3 shows the calculated horizontal intensity distribution for the HERA profile monitor ($x_c = 5.3$ mm, $\hat{p} = 6216$ mm), assuming a magnification $\hat{V} = 1$ and a point source located in the origin of the source plane. The advantage to use monochromatic light is clear to see: the intensity distribution for the larger wavelength interval is smoothed out, leading to an increased contribution of the diffraction broadening.

In order to quantify the horizontal diffraction broadening it is possible to fit a normal distribution at the central part of the calculated intensity profiles. For $\lambda = 450$ nm this gives a value of $\sigma_{x,d} = 95.2$ μm which is comparable to the result from the approximative formula given in Ref. [2] $\sigma_{x,d}^{app} = 1.39156 \lambda (2\pi x_c/\hat{p} \sqrt{2 \ln 2})^{-1}$, which leads to a value of 99.3 μm . At the other hand the comparison of these values with the “classical” expression of diffraction broadening from a slit aperture which is defined by the first minimum $x_{min} = \pi$ of the $\text{sinc}^2 x$ distribution results in $\sigma_{x,d}^{lap} = \frac{1}{2} \lambda / (x_c/\hat{p}) = 249.8$ μm , which is much larger than the values quoted above.

While in the fit procedure only the central part of the distribution is considered, i.e. the oscillating tails are not taken into account, the determination of the diffraction broadening based on the first order minimum is a rough estimation which overestimates the influence. Therefore in the next step the influence on the measured beam profile was investigated in order to specify a value for the resolution broadening. For this purpose the intensity distribution $I_x(x') = |F_x(x')|^2$ with $F_x(x')$ according to Eq.(3) was convoluted with the normal distributed horizontal beam profile, and the width of the resulting distribution was determined by fitting a normal distribution. From the derived width an “effective” value for the horizontal diffraction resolution can be deduced by quadratical subtraction of the beam size σ_x , leading to a value of $\sigma_{x,d} = 187.9$ μm which is used to correct the contribution of the diffraction broadening.

Vertical Distribution. In vertical direction the inherent angular distribution of SR light is normally the limiting factor. The amplitude distribution of the electric field is

given by

$$f_{y,\sigma}(\xi) = A_\sigma \frac{\hbar\omega}{2\hbar\omega_c} (1 + \xi^2) K_{2/3} \left[\frac{\hbar\omega}{2\hbar\omega_c} (1 + \xi^2)^{3/2} \right] \quad (4)$$

$$f_{y,\pi}(\xi) = A_\pi \frac{\hbar\omega}{2\hbar\omega_c} \xi \sqrt{1 + \xi^2} K_{1/3} \left[\frac{\hbar\omega}{2\hbar\omega_c} (1 + \xi^2)^{3/2} \right] \quad (5)$$

(see e.g. [4]) with $\xi = \gamma v = \gamma v/p$ the reduced vertical emission angle. $f_{y,\sigma}$ is the polarization component in the orbit plane, $f_{y,\pi}$ the perpendicular one. The amplitudes A_σ, A_π are independent on the emission angles u, v and can be disregarded for the integration in Eq.(1).

However, in the case of off-axis observation the lower integration limit in Eq.(1) is defined by the position of the light extracting mirror bottom edge y_m , i.e. $\xi_{min} = \gamma y_m / \hat{p}$, and the field distribution in the image plane is determined by

$$F_{y,\sigma/\pi}(y') = \frac{p}{\gamma} \int_{\xi_{min}}^{+\infty} d\xi f_{y,\sigma/\pi}(\xi) \exp(-i \frac{k p}{\gamma p'} \xi y'). \quad (6)$$

In Fig. 4 calculated vertical intensity distributions $I_y(y') = |F_y(y')|^2$ with F_y according to Eq.(6) are shown, assuming a magnification $V = p'/p = 1$. For mirror positions $y_m \leq -10$ mm there is no more change in the shape of the distributions. This value corresponds formally to the case $\xi_{min} = -\infty$, i.e. the conventional on-axis observation which is investigated in Refs. [1, 2]: the distribution of the σ polarization component has a narrow shape which can be described by a normal distribution while the one of the π component has a minimum on-axis. If the mirror is moved upward, the width of the σ polarization component is continuously broadened. With increasing y_m the on-axis minimum of the

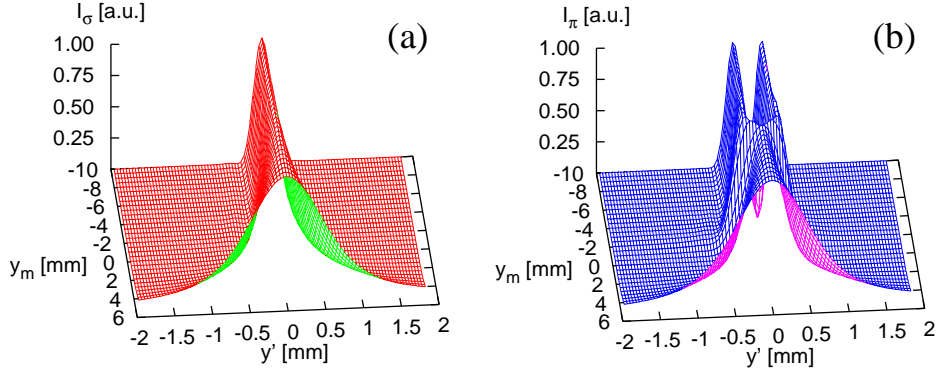


FIGURE 4. Diffraction limited vertical single electron intensity distribution in the image plane as function of the light extracting mirror bottom edge y_m in the case of σ (a) and π (b) polarization. $y_m < 0$: bottom edge is below the beam axis. The intensity is normalized to it's maximum value at each mirror position.

π component is smeared out and the shape of both polarization component distributions becomes more and more similar.

In order to quantify the contribution of the vertical diffraction broadening, the calculated intensity distributions $I_y(y')$ in Fig. 4 was convoluted with the vertical beam profile, assuming a normal distribution. The “effective” vertical resolution broadening was derived in a similar way than for the horizontal distribution by fitting the convoluted profile with a normal distribution with subsequent quadratical subtraction of the beam size σ_y . The results are plotted as function of y_m in Fig. 5(a) for both polarization states.

According to that, the contribution of the σ polarization component is continuously increasing with increasing y_m . Anyhow, if $y_m \leq 0$ mm the usage of this polarization component will lead to a better resolution than the usage of the π polarization. For larger mirror positions the resolution becomes independent on the polarization state.

In Fig. 5(b) the measured total width of the vertical beam profile is shown, including resolution broadening effects due to diffraction and depth of field. The measured beam size strongly reflects the influence of the vertical diffraction broadening as expected from Fig. 5(a).

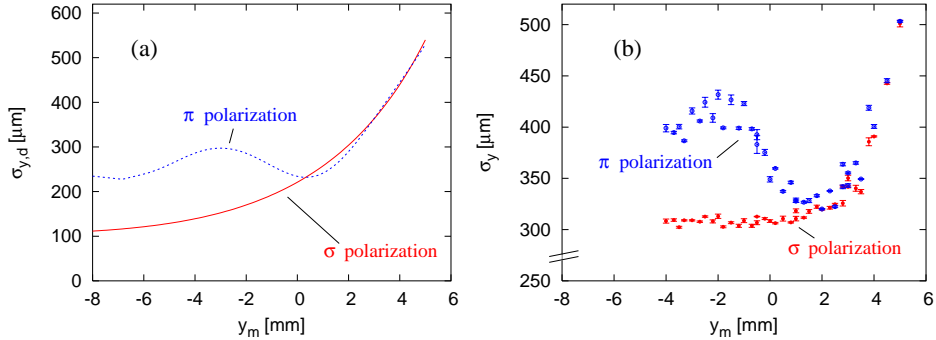


FIGURE 5. (a) Calculated contribution of the vertical diffraction broadening as function of the light extracting mirror bottom edge y_m . (b) Measurement of the vertical beam profile width as function of y_m , including resolution broadening contributions due to diffraction and depth of field.

Additionally, Fig. 6 shows screen shots of measured beam spots for two different mirror positions and both polarization states. While for $y_m = -4.3$ mm the measured vertical beam size for σ polarization is much smaller than for π polarization, they become independent on the polarization state for large y_m as expected from the calculations presented in Fig. 5(a).

For the HERA profile monitor the mirror position is chosen as $y_m = +2$ mm. This value is a compromise between a reasonable value for heat load and a sufficient vertical resolution.

The calculated resolutions in Fig. 5(a) show again larger deviations compared to the standard formula for vertical diffraction broadening, $\sigma_{y,d}^{app} = \frac{1}{2}\lambda/\Psi = (\frac{\pi}{6}\lambda^2\rho)^{1/3} = 400 \mu\text{m}$, with Ψ the typical SR opening angle and ρ the magnet bending radius. Apart from the aspect of off-axis observation this formula overestimates the resolution broadening drastically. Therefore calculations based on the standard formula are more a rough estimation than a precise calculation of the SR diffraction limited resolution.

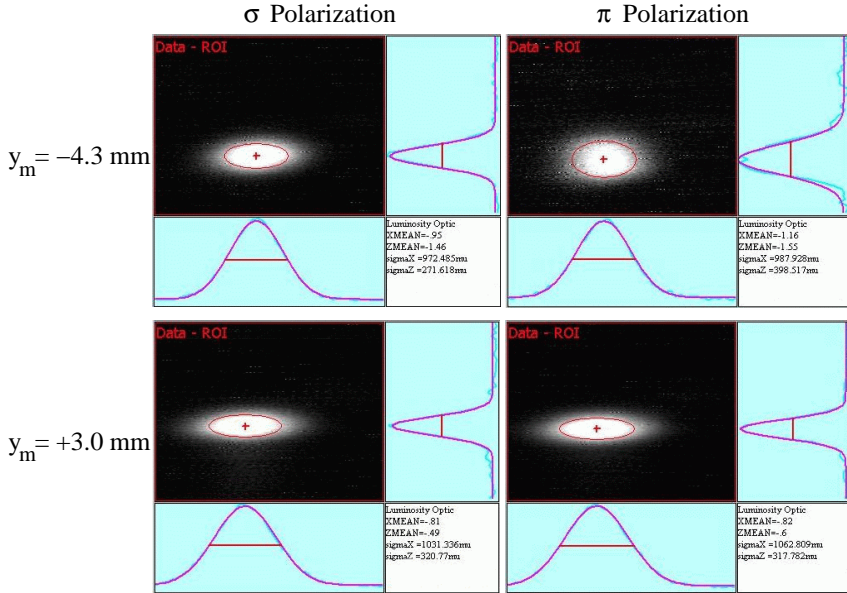


FIGURE 6. Screen shots of measured beam spots for two different mirror positions and both polarization states. The beam image is shown together with the projections onto the horizontal (x) and vertical (z) axis. By means of a fit the beam positions ($XMEAN$, $ZMEAN$) are determined together with the widths in both planes. Note that the range of interest (ROI) was chosen different for both mirror positions.

FIELD-DEPTH LIMITED RESOLUTION

The calculations for the depth of field are based on the considerations in Ref. [2]. The particle trajectory is divided in small slices which are treated as point sources, and their angular distributions are summed up as if they emit incoherently. The SR source region consists of a number of slices that are focused by the lens at different at various distances from the image plane (x', y').

In first order imaging theory, a point with emission angle α which is a distance s away from the vertical source plane y_0 (i.e. a single slice), is imaged onto a point y' in the image plane according to $y' = -\frac{p'}{p}(y_0 + s \alpha)$. Under the simplified assumption that y_0 and α are normal distributed in the source plane with widths σ_y resp. σ_α , the distribution of y' in the image plane is also normal distributed with width $\frac{p'}{p} \sqrt{\sigma_y^2 + (\rho \vartheta \sigma_\alpha)^2}$. In this relation the orbit coordinate was replaced by $s = \rho \vartheta$ according to Fig. 1.

Summing up the contributions along the particle trajectory results in the vertical intensity distribution in the image plane

$$I_{y,fd}(y') = I_0 \int_{-\vartheta_{lim}}^{+\vartheta_{lim}} \frac{p\rho h(\vartheta) d\vartheta}{p' \sqrt{2\pi} \sqrt{\sigma_y^2 + (\rho \vartheta \sigma_\alpha)^2}} \exp \left[-\frac{(py')^2}{2p'^2 \{\sigma_y^2 + (\rho \vartheta \sigma_\alpha)^2\}} \right] \quad (7)$$

with I_0 a normalization constant and $\vartheta_{lim} = x_c/\hat{p} + \Psi$ the accepted angle, taking into account the aperture limitation given by the extraction mirror together with the SR typical opening angle. The function $h(\vartheta)$ accounts for the amount of light extracted by the mirror from different trajectory slices:

$$h(\vartheta) = \frac{1}{2} \left[\operatorname{erf} \left(\frac{x_c/\hat{p} - \vartheta}{\sqrt{2}\sigma_\vartheta} \right) - \operatorname{erf} \left(-\frac{x_c/\hat{p} + \vartheta}{\sqrt{2}\sigma_\vartheta} \right) \right] \quad (8)$$

with σ_ϑ the width of the normally distributed horizontal emission angle. Eq. 7 holds also for the horizontal intensity distribution with the exception that the intensity distribution from each slice is shifted by $\Delta x = \rho \vartheta^2$ against the position at $s = 0$, taking into account the curvature of the trajectory which results in an additional broadening.

Calculations based on this model lead to a resolution broadening of $\sigma_{y,fd} = 154 \mu\text{m}$ for the vertical and $\sigma_{x,fd} = 292 \mu\text{m}$ for the horizontal intensity distribution. These values are again smaller than the ones according to standard approximations (see e.g. Refs. [1, 5]), $\sigma_{y,fd}^{app} = \rho x_c/\hat{p}\Psi = 185 \mu\text{m}$, resp. $\sigma_{x,fd}^{app} = \rho (x_c/\hat{p})^2 = 440 \mu\text{m}$. The deviation in horizontal direction becomes even larger because the approximative contribution due to the orbit curvature (see e.g. Ref. [5]) $\sigma_{x,c} = \rho/2 (x_c/\hat{p})^2 = 220 \mu\text{m}$ has to be taken into account.

SUMMARY

In the present article a beam profile monitor system using visible SR radiation from a bending magnet at the HERA storage ring has been described. By use of models for diffraction and depth of field effects described above it is possible to determine the actual beam rms sizes. The calculations show large discrepancies in comparison to the ones based on standard formulas which estimate resolution broadening. Moreover special attention is drawn to the influence of off-axis observation which smears out the vertical resolution additionally. While the absolute values of the measured beam sizes deviate up to now from their design values (reason seems to be a discrepancy to the particle beam design optics), the monitor is already now a versatile tool for studies of relative changes in the beam emittances.

REFERENCES

1. A. Hofmann and F. Méot, Nucl. Instr. Meth. **203** (1982) 483.
2. Å. Andersson and Juri Tagger, Nucl. Instr. Meth. **A 364** (1995) 4.
3. A. S. Fisher *et al.*, in Proceedings of EPAC96, p.1734.
4. A. Hofmann, Proceedings of the CAS 98-04.
5. J. A. Clarke, *A Review of Optical Diagnostics Techniques for Beam Profile Measurements*, EPAC 94, www.astec.ac.uk/preprints/epac94/JAC-Profile_paper.pdf.